An Update to the HRC-I Quantum Efficiency Model

J. Posson-Brown (CXC/SAO)
R. H. Donnelly (CXC/SAO) D. Pease (CXC/SAO)

27 October 2003

Abstract

We present an update to the HRC-I MCP quantum efficiency (QE) model based on calibration observations of the blazar PKS 2155-304 taken in November 2002. The HRC-I observation of PKS 2155-304 was taken between two HRC-S/LETG observations of the source. These HRC-S/LETG observations allowed us to model the source and predict a count rate for the HRC-I observation. We found that this predicted rate is ~7% lower than the observed rate. Therefore, we have increased the MCP QE model of the HRC-I in the energy range 0.277 - 1.0 keV where PKS 2155-304 radiates strongly and where we previously had no flight data. With this update, the discrepancy between observed and predicted count rates for PKS 2155-304 drops to ~1%. Outside of 0.277 - 1.0 keV, the predictions of the current QE model (v. 2.1) are consistent with observations of the other calibration sources - HZ 43, Cas A, and G21.5-0.9.

We also report on the evolution of the HRC-I QE over time as monitored by HZ 43, Cas A, and G21.5-0.9 since October 1999.

Adjusting the QE Model

The on-axis quantum efficiency is monitored with regular calibration observations of three sources which radiate in generally distinct regimes: HZ 43 (below 0.2 keV), Cas A (0.7-2.5 keV), and G21.5-0.9 (above 1 keV). Observations of these sources have allowed us to test and constrain the QE model

in the respective energy ranges. However, prior to the PKS 2155-304 observations, we had no flight data in the energy range 0.2-0.7 keV. The PKS 2155-304 observations were done to test the QE model in this range.

For each of the two PKS 2155-304 observations taken with the HRC-S/LETG, we extracted a spectrum and fit a power-law model. The parameters for the fits are shown in Table 1. The consistency (within errors) of the fit parameters for the "before" and "after" observations indicates that the source was stable over the duration of the three observations. We used the average value of the power-law index, $\Gamma = 2.375$, when predicting a count rate for the HRC-I observation. The predicted rate we derived by convolving the source model with the v2.1 HRC-I QE model, and current HRMA effective area, UVIS transmission, and LETG efficiency models, is 1.58 cts/s.

Our observed rates are taken from Level 1 event lists which have been filtered on the good time intervals (GTIs) provided in the standard filter files. For the HRC-I PKS 2155-304 observation, we find an observed count rate of 1.70 ± 0.01 cts/s. This is 7% higher than the predicted rate. For the other calibration sources, the observed and predicted count rates agree to within 4% or less.

We increased the QE model in the range 0.277 to 1.0 keV with a smooth quadratic scale factor to avoid introducing artificial features. With this increase, the pre dicted rate for PKS 2155-304 agrees with the observed rate to within $\sim$1%. For the other three sources, the rates predicted by the updated model agree with observed rates to within 3% or less. Table 2 shows the observed rat es, predicted rates with QE model v2.1, and predicted rates with the updated QE model. The percent difference between the observed and predicted rates for each source is shown in parenthesis after the predicted rates.

The updated QE model is shown in Figure 1 with its error envelope in blue. The v2.1 QE model and associated error are overplotted, and the scale factor (minus one) is shown below the model. An updated effective area (EA) model was made by convolving the updated QE model with the most recent UVIS transmission and HRMA effective area models. This updated EA model for the HRC-I is shown in Figure 2, with its associated error envelope. The v2.1 EA model and error are overplotted.

ObsID	nH (atoms/cm^2)	Γ	normalization
3709 (before HRC-I)	1.36e20	2.35 $\pm$ 0.05	0.027 $\pm$ 0.002
4406 (after HRC-I)	1.36e20	2.40 $\pm$ 0.05	0.027 $\pm$ 0.002

Table 1: Parameters from power law models fit to HRC-S/LETG PKS 2155-304 observations done before and after the HRC-I PKS 2155-304 observation

Source	Energy Range	Observed Rate	Pred w/ QE v2.1	New Pred
	keV	cts/s	cts/s	cts/s
HZ 43	$\leq$ 0.2	4.35 $\pm$ 0.05	4.29 (1.38%)	4.29 (1.38%)
PKS 2155-304	0.2 - 2.5	1.70 $\pm$ 0.01	1.58 (7.06%)	1.68 (1.18%)
Cas A	0.7 - 2.5	89.19 $\pm$ 1.60	85.77 (3.83%)	86.58 (2.93%)
G21.5-0.9	$\geq$ 1.0	0.61 $\pm$ 0.02	0.62 (1.64%)	0.62 (1.64%)

Table 2: Observed, current (v2.1), and new predicted count rates. The percentages in parenthesis after the predicted rates are the differences from the observed rates.

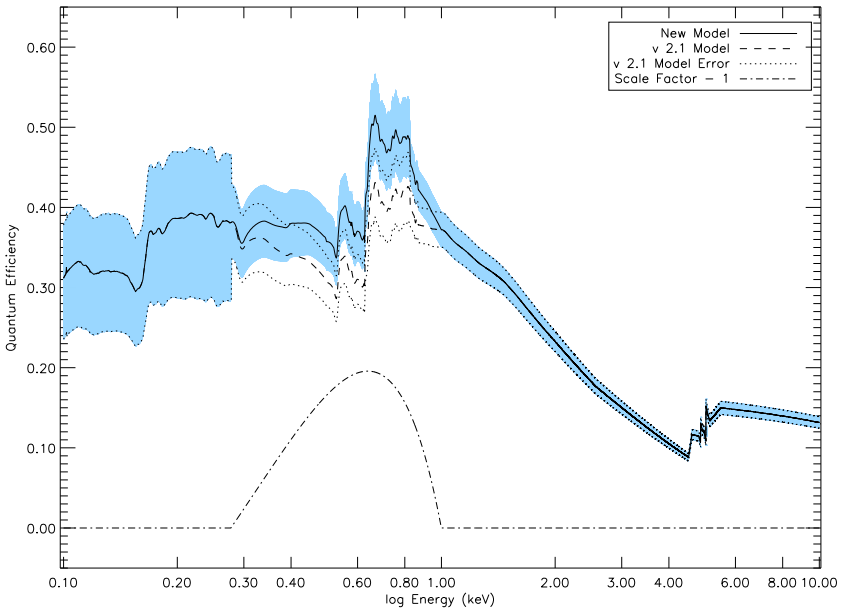

Figure 1: The new QE model and error envelope. The current QE model (v2.1) and error are overplotted, and the scale factor (minus 1) is shown below.

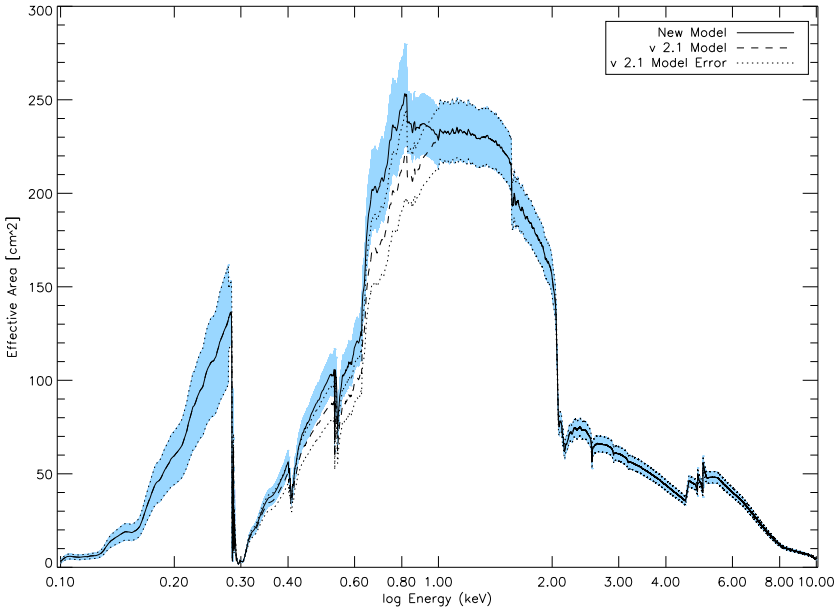

Figure 2: The updated EA model and error envelope. The current model (v2.1) and error are overplotted.

Source	Energy Range	Best Fit Slope	QE Decline
	keV	$\frac{cts/s}{month}$	%
HZ 43	≤ 0.2	-5.11e-4 $\pm$ 4.66e-4	1.8 $\pm$ 1.6
Cas A	0.7 - 2.5	-4.68e-4 $\pm$ 2.86e-4	1.2 $\pm$ 0.7
G21.5-0.9	≥ 1.0	-6.05e-5 $\pm$ 4.33e-4	0.3 $\pm$ 1.9

Table 3: Best fit slopes with 1 σ error and resulting estimates for percentage of decline in QE.

Monitoring QE Evolution

To monitor the quantum efficiency of the HRC-I, we compare count rates from observations of HZ 43, Cas A, and G21.5-0.9 taken over the past few years. We derived count rates from Level 1 event lists filtered on the nominal good time intervals provided in the standard filter files. For some of the G21.5-0.9 and Cas A observations, additional time filtering was done to exclude time intervals affected by telemetry saturation.

Figure 3 shows plots of count rates versus time for the three sources. The count rates shown have been normalized to the mean rate for each source, and the error bars represent the statistical error. In each panel, the solid line represents a constant value of one, and the dashed line shows the linear least-squares fit to the data. The dotted lines show the range of slopes allowed by the standard deviation of the best-fit slope. The best-fit slopes and standard deviations for each source, and resulting percentage of decline in QE, are given in Table 3. There is weak evidence for a small decline in QE as witnessed by HZ 43 and Cas A, and no evidence for a QE decline from the G21.5-0.9 observations.

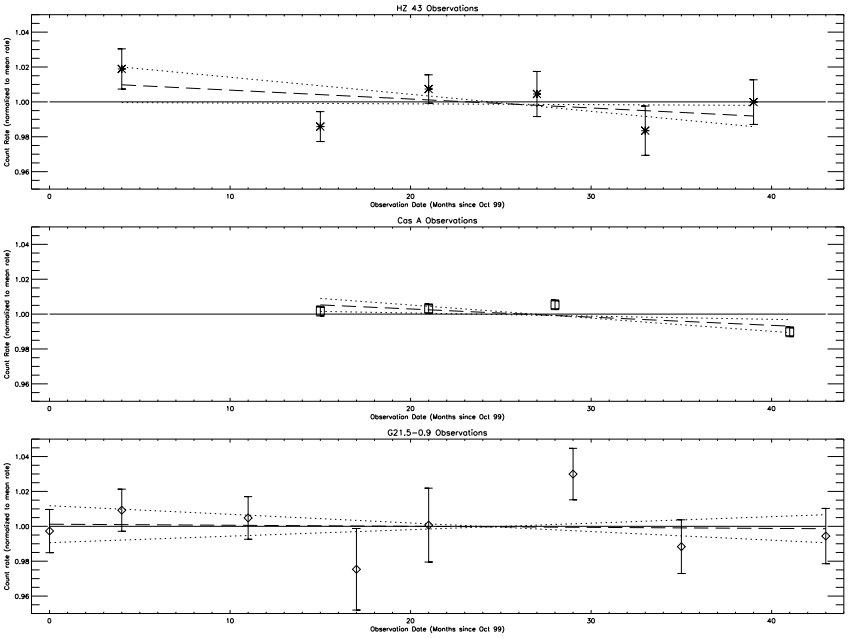

Figure 3: Normalized count rates versus time for HZ 43 (top), Cas A (middle), and G21.5-0.9 (bottom).